

# Deposition of Lignin Particles on the Surface of Treated and Non-Treated Active Carbon

Nagore Izaguirre<sup>a</sup>, Xabier Erdocia<sup>b</sup>, Rodrigo Llano-Ponte<sup>a</sup>, Jalel Labidi<sup>a,\*</sup>

<sup>a</sup>Chemical and Environmental Engineering Department. University of the Basque Country UPV/EHU, Plaza Europa, 1, 20018. San Sebastian, Spain

<sup>b</sup>Department of Applied Mathematics, University of the Basque Country (UPV/EHU), Rafael Moreno "Pichichi" 3, Bilbao, 48013, Spain  
[jalel.labidi@ehu.es](mailto:jalel.labidi@ehu.es)

Carbons are sustainable and highly abundant materials with prospects of taking over the currently used metallic or inorganic materials, whose widespread employment entail questionable obstacles due to their scarcity and difficult extraction. Carbon materials are physicochemically stable, as well as having other interesting properties such as electrochemical conductivity, as a result of their simple yet efficient structure. Creating composites with these materials can promote even further their employment in a variety of applications. This is especially interesting when these other materials are also environmentally sustainable, such as, for instance, lignin. Even though it is currently considered industrial waste, lignin has many interesting properties, like high aromaticity and redox-active moieties. Combining these two green materials a compound with enhanced properties can be obtained, interesting for energy storage applications, as the non-faradaic nature of carbon combines with the faradaic nature of the redox moieties of lignin. Ultrasonic forces (US) were employed for the surface deposition of both industrially available Kraft lignin (KL) and organosolv lignin extracted on a laboratory scale (OL). The commercially available active carbon (AC) was chemically treated to observe the influence of the deposition efficacy and morphological variations. Moreover, the influence of the lignin type was also studied. These materials were characterized by Fourier Transformed Infrared Spectroscopy (FTIR), Atomic Force Microscopy (AFM), Dynamic Light Scattering (DLS), and Thermogravimetric Analysis (TGA). These methods were effective for the verification of both the chemical modification of the carbon and the deposition of lignin, being able also to determine differences in these phenomena depending on the surface of the carbon and lignin type employed.

## 1. Introduction

Carbon materials have exceeding versatility for numerous applications. They have plausible potential to substitute the currently used materials like metals and petroleum-derived compounds, whose scarcity and lack of sustainability provoke the urge for their replacement. Furthermore, large quantities of carbons can be produced sustainably and at low cost, since they can be successors of wastes and naturally abundant materials like lignocellulosic ones (Thomas et al., 2021).

The wide spectrum of applications covered by carbon materials ranges from photochemical catalysts for solar energy conversion to chemical energy (Lin et al., 2023). In addition, it can be employed for CO<sub>2</sub> reduction and water splitting (Sohail et al., 2022), contaminant removal and water purification (Hu et al., 2022), electrochemical sensing platform (Umapathi et al., 2022) or electrochemical energy storage like batteries and supercapacitors (Sultanov et al., 2023).

The morphology and porosity of carbonaceous materials are key factors that greatly influence their applicability and performance (Akbari Beni et al., 2020). One type of carbon that has been gaining attention due to its porosity and high surface area is activated carbon. They are highly tuneable, with both physical and chemical modification procedures to approach the properties desired for each targeted application (Yan et al., 2023). One of the most common modifications is the activation of the carbon surface through nitric acid (HNO<sub>3</sub>). This way, oxygen-containing groups are introduced in the porous surface, along with other nitrogen

functional groups, the last ones in smaller amounts. This functionalization with N and O has been reported to show the best results for electrochemical applications (Ternero-Hidalgo et al., 2016). Moreover, the creation of more active sites also enables further modification of the surface of the carbon, for example, by adding redox-active molecules.

The addition of redox-active molecules is especially interesting when enhanced electrochemical properties are desired since both faradaic and non-faradaic processes take part. Carbon materials are usually non-faradaic, but with the addition of redox-active molecules, the obtained material can combine both properties and enhance the final efficiency.

An interesting molecule with redox-active moieties is lignin. It is, moreover, considered to be a key compound for the obtention of more environmentally friendly products, due to its high abundance in nature, easy obtaining, and complex structure and properties. It is the second most abundant polymer found in nature, after cellulose, as it is one of the main components of all lignocellulosic materials. It is highly aromatic and complex, with high heterogeneity. Depending on the extraction method, raw material, and other environmental factors, physicochemical properties differ. Kraft lignin is the most abundant lignin found, due to the widely employed method in paper and pulp industries. Adversely, organosolv lignin is the lignin type considered the most environmentally sustainable, since all lignocellulosic components are targeted as products, and a multiproduct biorefinery process is designed for that (Schutyser et al., 2018).

Therefore, by combining these two materials a compound with synergized properties can be obtained, with enhanced properties able to substitute more advanced materials. Since the products used are sustainable, it is also important to design a sustainable process for compound obtaining, without the use of harsh reactions and energetically demanding processes. Ultrasound (US) irradiation is widely employed in sustainable processes. Its irradiation is based on acoustic cavitation, and correctly irradiated liquids can create bubbles that will then expand and collapse with each other, inducing the formation of radicals and the fulfilment of the reaction at lower energetic inputs and shorter periods than in conventional procedures (Suslick et al., 1999).

This study presents the physicochemical and morphological study of the compounds synthesized, based on commercial active carbon and lignin-derived from both industrial waste and lab-scale biorefinery processes. Moreover, the study of the active carbon treatment was carried out to determine its efficacy in the subsequent lignin deposition. It was concluded that the carbon treatment was successful in enhancing the lignin particles deposited on the surface and that a more functionalized lignin, with a smaller molecular weight, was desirable for its optimal yield.

## 2. Materials and Methods

### 2.1 Materials

KL was precipitated from the kraft liquor and OL was extracted from Eucalyptus sp. chips, both provided by Papelera Zikuñaga (Hernani, Gipuzkoa) and characterized in a previous work (Izaguirre et al., 2022). Granulated active carbon (AC) (7440-44-0, Panreac) was purchased. AC was treated with nitric acid (HNO<sub>3</sub>) (65%, 7697-37-2, Panreac). Lignin was deposited with an acetone solution (67-64-1, technical, Scharlab), a 0.22 μm nylon filter was used for the obtention of the solid, and hydrochloric acid (HCl) (37%, 7647-01-0, Panreac) and sodium hydroxide (NaOH) (1310-73-2, Panreac) were used for the titrant solution preparation for the DLS.

*Table 1: Physicochemical properties of the Kraft lignin (KL) and Organosolv lignin (OL) used in this work (Izaguirre et al., 2022)*

	KL	OL
M <sub>w</sub> (g/mol)	3167	5800
PI	2.91	4.44
Aliphatic OH content (mmol/L)	0.43	1.44
Phenolic OH content (mmol/L)	1.62	1.30
S (%)	51.0	54.88
G (%)	44.90	42.33
H (%)	4.11	2.80
T <sub>50</sub> (°C)	430	370
T <sub>g</sub> (°C)	129	140

## 2.2 Treatment of active carbon (TAC)

Granulated active carbon was milled and added to concentrated  $\text{HNO}_3$ . The solution was then heated in a bath oil at  $80\text{ }^\circ\text{C}$  and stirred at 200 rpm for 2 h. The solution was filtered with a  $0.22\text{ }\mu\text{m}$  nylon filter and washed with DI water until neutral pH. The product was dried at  $60\text{ }^\circ\text{C}$  overnight.

## 2.3 Deposition of lignin into the surface of the carbon

Kraft lignin and organosolv lignin were deposited onto the untreated and treated active carbon (AC and TAC) following the procedure described elsewhere (Zhou et al., 2019). For that, 200 mg of lignin and 20 mg of carbon were added to a 40 mL acetone/ $\text{H}_2\text{O}$  solution (7:3 v/v) and immersed in an ultrasonic bath for 15 minutes. The solution was centrifuged at 8000 rpm for 15 minutes. The solid was washed with 40 mL of the same solvent mixture, sonicated for 15 minutes, and centrifuged in the same conditions. The solid was dried at  $60\text{ }^\circ\text{C}$  overnight. Thus 4 composites were obtained AC-KL, AC-OL, TAC-KL AND TAC-OL

## 2.4 FTIR

FTIR spectra were recorded with the Spectrum Two Spectrometer by Perkin Elmer to observe the chemical modifications of active carbon and verify the deposition of lignin on the surface of the material. The wavenumber range was set from  $4000$  to  $600\text{ cm}^{-1}$ , with a resolution of  $4\text{ cm}^{-1}$  and 24 scans.

## 2.5 DLS

A ZetaSizer Ultra (Malvern Panalytical) equipped with a He-Ne laser source ( $\lambda=633\text{ nm}$ ) and a scattering angle of  $173^\circ$  was used for the particle size and Z potential characterization. Samples were dispersed in 0.5 wt% concentration in deionized water. To obtain a homogeneous dispersion the samples were stirred overnight and immersed in an ultrasound bath for 30 min (Gupta et al., 2015). The samples were measured in a variety of pH-s, from 2 to 10, adjusting the pH with an automatic titrator and using solutions of 0.5M HCl, 0.1M HCl, and 0.5M NaOH as titrants.

## 2.6 AFM

AFM images of the sample surfaces were recorded in tapping mode, using a Nanoscope IIIa scanning probe microscope (Multimode TM Digital instruments) and a cantilever/silicon probe, generating an integrated force. The cantilever's length was  $125\text{ }\mu\text{m}$ , and the tip radius was 5–10 nm. 0.035 %wt. aqueous dispersions were prepared, and indirect ultrasonication was applied. A drop of the sample solution was deposited in the holder and analyzed when dried.

## 2.7 TGA

Thermogravimetric analyses were performed using a TGA/DSC3+ by Mettler-Toledo. Analyses of the thermal behavior of the samples from RT to  $1000\text{ }^\circ\text{C}$ , with a heating rate of  $10\text{ }^\circ\text{C}/\text{min}$  were carried out under inert conditions (Liu et al., 2019).

## 3. Results

### 3.1 FTIR

FTIR spectra were recorded for the verification of the  $\text{HNO}_3$  treatment of active carbon and the deposition of the lignins on the surfaces of the carbons. Figure 1 shows the spectra of active carbon (AC) and  $\text{HNO}_3$ -treated active carbon (TAC), as well as the composites obtained (AC-KL, AC-OL, TAC-KL, and TAC-OL) and the lignins (KL and OL). From the spectra, an increased intensity can be observed from AC to TAC in the bands at  $1700$  and  $1100\text{ cm}^{-1}$ , wavelengths attributed to C=O stretching and C-N stretching respectively, verifying the oxidation reaction and functionalization of the carbon surface with O and N. The characteristic bands of the lignins (KL and OL) and both carbons (AC and TAC), as well as their combination of bands at AC-KL, AC-OL, TAC-KL, and TAC-OL, corroborate that the treatment of the carbon enhances the deposition of further molecules, in this case, lignin, since the characteristic bands attributed to lignin are more intense in TAC-KL and TAC-OL than in AC-KL and AC-OL: O-H stretching band at  $3400\text{ cm}^{-1}$ , C=O stretching at  $1700\text{ cm}^{-1}$ , COO<sup>-</sup> stretching at  $1620\text{ cm}^{-1}$ , and C-O-C stretching at  $1200\text{ cm}^{-1}$  (Ren et al., 2013; Suktha et al., 2015; Zhou et al., 2019).

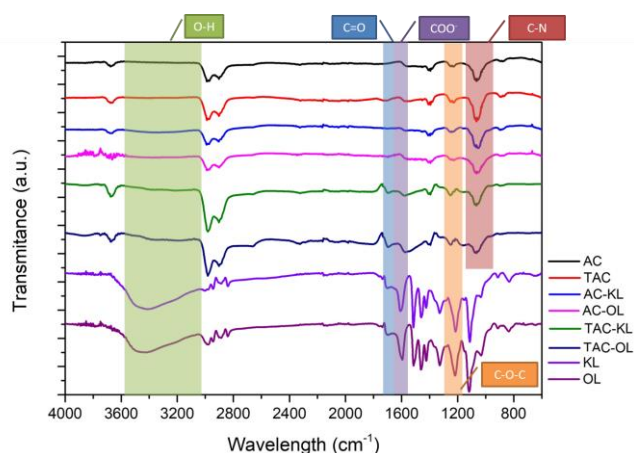


Figure 1. FTIR spectra of AC, TAC, AC-KL, AC-OL, TAC-KL, TAC-OL, KL, and OL

### 3.2 Particle size and Z potential

Z potential (mV) and Particle size (nm) of the samples were recorded. 0.5 %wt. dispersions were prepared, and pH was varied from 2 to 10. Values were recorded at every pH interval. Z potential is related to the surface charge of the molecules. The higher the ZP value a molecule has (both positive and negative) the more stable it is. Moreover, pH also affects particle size. Depending on the medium of the solvent (acidic or basic), the functional groups of the particle's surface may or may not interact with the solvent or ion within, creating bigger or smaller particle suspensions. Z potential values higher than 30 mV (or lower than -30 mV) are considered to show incipient stability (shown in blue in Figure 2). Values higher than 40 mV are considered to have good stability (shown in green in Figure 2). From the results obtained, higher pH values enhance the stability of the particles, and when the pH value reaches 2, the ZP values of all sample decrease to almost 0 mV, and particles precipitate. AC particles are the most unstable, having a low ZP in all the pH range. When reacted with  $\text{HNO}_3$  (TAC) stability improves considerably, probably due to the addition of functional groups that interact with  $\text{H}_2\text{O}$  molecules. However, the particle size also increases drastically. This might be due to the interactions that happen between the functional groups of TAC between them and with the medium. Carbon particles stabilize even further with the deposition of lignin, especially with OL. Apart from being the most stable, AC-OL and TAC-OL were the smallest in size, followed by AC-KL and TAC-KL, which were slightly bigger. Finally, TAC particles were the biggest ones at high pHs (due to intermolecular interactions created with the solvent) but decreased to around 1000 nm when precipitated at pH 2.

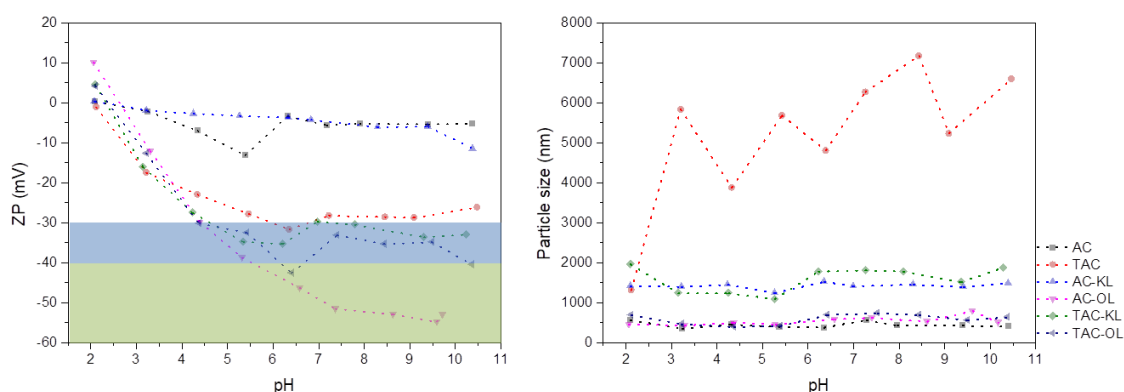


Figure 2. Z Potential and Particle size of the samples, in a pH range of 2 to 10

### 3.3 AFM

To understand the morphological properties of the samples, AFM microscopy experiments were carried out. Images of 500x500 nm were obtained and shown in Figure 3. Differences in the surfaces of the samples can be observed along with the modifications on the surface due to the treatment and lignin deposition. AC already had a porous surface, where lignin particles deposited after the treatment with US forces. With the  $\text{HNO}_3$

treatment, however, a variation on the surface could also be observed, where the porous structure maintained with considerably smaller-sized pores and an increment in the roughness. These surface properties and the higher functionalization, enabled a further deposition of the lignins, verified by the AFM the higher quantity of lignin particles in TAC molecule surfaces. In terms of the difference between KL and OL, KL seems to be more efficient, since a rougher surface seems to be obtained. This probably is related to the fact that KL molecules are smaller in size and weight, and are more functionalized with OH groups than organosolv lignin, which has a much milder extraction procedure and therefore, bigger molecules are obtained, hindering their ability to deposit on the pores and react with the active sites.

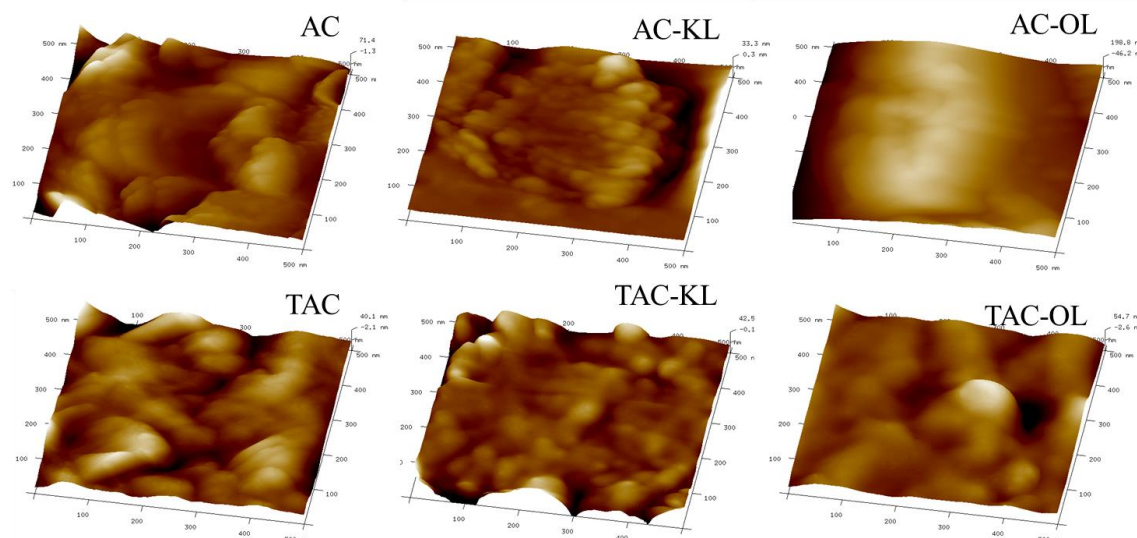


Figure 3. AFM images of AC, AC-KL, AC-OL, TAC, TAC-KL, and TAC-OL

### 3.4 TGA

Thermogravimetric analyses (TGA) were carried out from room temperature to 1000 °C. Similar trends could be observed, being AC-KL the only exception. A drop around 400 °C is visible, T which corresponds to the main degradation temperature of lignin. Therefore, it can be concluded that the sample contained KL residue since this drop is significantly less prominent in other samples. Even though the incorporation of lignin is verified by FTIR, there are no effects on the degradation of the composites, since there is no drop around 300-400 °C, the usual T in which lignin gets degraded. This probably is due to the low amount of lignin constituting the overall material. Samples showed high thermal stability, maintaining more than half of their total weight even at 1000 °C, a common characteristic of carbon materials that are not negatively affected by the modification procedures carried out.

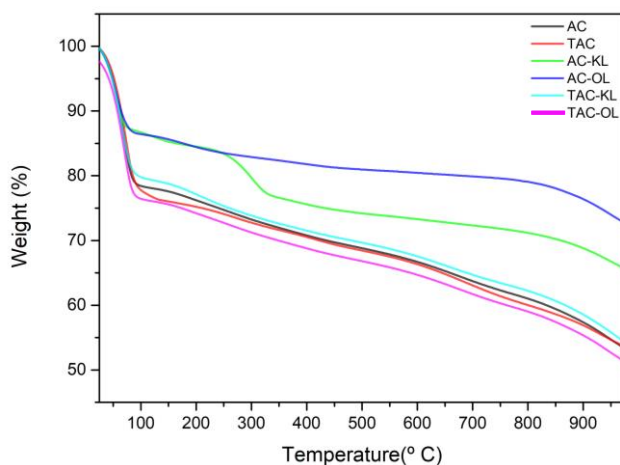


Figure 4. TG curves of samples from RT to 1000 °C

#### 4. Conclusions

Treatment of active carbon was successful for its surface activation. More functional groups were present after the reaction with HNO<sub>3</sub>, and enhanced deposition of lignin could be observed after the US treatment. These treatments (reaction with HNO<sub>3</sub> and US irradiation) were effective for obtaining stable particles at neutral and basic pH, and relatively small particle sizes, attractive properties for their employment in energy storage applications or as adsorbents. Moreover, rough and more porous surfaces were obtained both when the AC was turned into TAC and lignins were deposited in AC and TAC.

#### Acknowledgments

The authors would like to acknowledge the financial support of the Basque Government (grant PIF19–183 and IT1498-22).

#### References

- Akbari Beni, F., Gholami, A., Ayati, A., Niknam Shahrak, M., Sillanpää, M., 2020. UV-switchable phosphotungstic acid sandwiched between ZIF-8 and Au nanoparticles to improve simultaneous adsorption and UV light photocatalysis toward tetracycline degradation. *Microporous Mesoporous Mater.* 303, 6–14.
- Gupta, A.K., Mohanty, S., Nayak, S.K., 2015. Synthesis, Characterization and Application of Lignin Nanoparticles (LNPs). *Mater. Focus* 3, 444–454.
- Hu, J., Zhao, L., Luo, J., Gong, H., Zhu, N., 2022. A sustainable reuse strategy of converting waste activated sludge into biochar for contaminants removal from water: Modifications, applications and perspectives. *J. Hazard. Mater.* 438, 129437.
- Izaguirre, N., Robles, E., Llano-Ponte, R., Labidi, J., Erdocia, X., 2022. Fine-tune of lignin properties by its fractionation with a sequential organic solvent extraction. *Ind. Crops Prod.* 175, 114251.
- Lin, H., Wu, J., Zhou, F., Zhao, X., Lu, P., Sun, G., Song, Y., Li, Y., Liu, X., Dai, H., 2023. Graphitic carbon nitride-based photocatalysts in the applications of environmental catalysis. *J. Environ. Sci. (China)* 124, 570–590.
- Liu, L., Solin, N., Inganäs, O., 2019. Scalable lignin/graphite electrodes formed by mechanochemistry. *RSC Adv.* 9, 39758–39767.
- Ren, T.Z., Liu, L., Zhang, Y., Yuan, Z.Y., 2013. Nitric acid oxidation of ordered mesoporous carbons for use in electrochemical supercapacitors. *J. Solid State Electrochem.* 17, 2223–2233.
- Schutyser, W., Renders, T., Van Den Bosch, S., Koelewijn, S.F., Beckham, G.T., Sels, B.F., 2018. Chemicals from lignin: An interplay of lignocellulose fractionation, depolymerisation, and upgrading. *Chem. Soc. Rev.* 47, 852–908.
- Suktha, P., Chiochan, P., Iamprasertkun, P., Wutthiprom, J., Phattharasupakun, N., Suksomboon, M., Kaewsongpol, T., Sirisinudomkit, P., Pettong, T., Sawangphruk, M., 2015. High-Performance Supercapacitor of Functionalized Carbon Fiber Paper with High Surface Ionic and Bulk Electronic Conductivity: Effect of Organic Functional Groups. *Electrochim. Acta* 176, 504–513.
- Sultanov, F., Mentbayeva, A., Kalybekkyzy, S., Zhaisanova, A., Myung, S.T., Bakenov, Z., 2023. Advances of graphene-based aerogels and their modifications in lithium-sulfur batteries. *Carbon N. Y.* 201, 679–702.
- Suslick, K.S., Didenko, Y., Fang, M.M., Hyeon, T., Kolbeck, K.J., McNamara III, W.B., Mdleleni, M.M., Wong, M., 1999. Acoustic cavitation and its chemical consequences. *Philos. Trans. R. Soc. A* 335–353.
- Ternero-Hidalgo, J.J., Rosas, J.M., Palomo, J., Valero-Romero, M.J., Rodríguez-Mirasol, J., Cordero, T., 2016. Functionalization of activated carbons by HNO<sub>3</sub> treatment: Influence of phosphorus surface groups. *Carbon N. Y.* 101, 409–419.
- Thomas, B., Geng, S., Sain, M., Oksman, K., 2021. cett-generation energy storage applications. *Nanomaterials* 11, 1–19.
- Umapathi, R., Venkateswara Raju, C., Majid Ghoreishian, S., Mohana Rani, G., Kumar, K., Oh, M.H., Pil Park, J., Suk Huh, Y., 2022. Recent advances in the use of graphitic carbon nitride-based composites for the electrochemical detection of hazardous contaminants. *Coord. Chem. Rev.* 470, 214708.
- Yan, H., Lai, C., Liu, S., Wang, D., Zhou, X., Zhang, M., Li, L., Li, X., Xu, F., Nie, J., 2023. Metal-carbon hybrid materials induced persulfate activation: Application, mechanism, and tunable reaction pathways. *Water Res.* 234.
- Zhou, B., Liu, W., Gong, Y., Dong, L., Deng, Y., 2019. High-performance pseudocapacitors from kraft lignin modified active carbon. *Electrochim. Acta* 320, 134640.